USCAP

ARTICLE

High levels of TIMP1 are associated with increased extracellular matrix stiffness in isocitrate dehydrogenase 1-wild type gliomas

Chun-Hua Luo[1], Yu Shi[1], Yu-Qi Liu[1], Qing Liu[1], Min Mao[1], Min Luo[1], Kai-Di Yang[1], Wen-Ying Wang[1], Cong Chen[1], Qin Niu[1], Ze-Xuan Yan[1], Jing-Ya Miao[1], Xiao-Ning Zhang[1], Hui Zeng[1], Lei Li[1], Xiu-Wu Bian[1]✉ and Yi-Fang Ping[1]✉

Glioma progression is accompanied with increased tumor tissue stiffness, yet the underlying mechanisms are unclear. Herein, we employed atomic force microscopy analysis to show that tissue stiffness was higher in isocitrate dehydrogenase (IDH)-wild type gliomas than IDH-mutant gliomas. Bioinformatic analyses revealed that tissue inhibitor of metalloproteinase-1 (*TIMP1*) was one of the preferentially upregulated genes in IDH-wild type gliomas as compared to IDH-mutant gliomas, and its higher expression indicated worse prognosis of glioma patients. TIMP1 intensity determined by immunofluorescence staining on glioma tissues positively correlated with glioma tissue stiffness. Mechanistically, *TIMP1* expression was positively correlated with the gene expression of two predominant extracellular matrix components, tenascin C and fibronectin, both of which were also highly expressed in IDH-wild type gliomas. By introducing IDH1-R132H-containing vectors into human IDH1-wild type glioma cells to obtain an IDH1-mutant cell line, we found that IDH1 mutation increased the *TIMP1* promoter methylation through methylation-specific PCR. More importantly, IDH1-R132H mutation decreased both the expression of TIMP1, fibronectin, tenascin C, and the tumor tissue stiffness in IDH1-mutant glioma xenografts in contrast to IDH1-wild type counterparts. Moreover, TIMP1 knockdown in IDH-wild type glioma cells inhibited the expression of tenascin C and fibronectin, and decreased tissue stiffness in intracranial glioma xenografts. Conclusively, we revealed an IDH mutation status-mediated mechanism in regulating glioma tissue stiffness through modulating TIMP1 and downstream extracellular matrix components.

Laboratory Investigation (2022) 102:1304–1313; https://doi.org/10.1038/s41374-022-00825-4

INTRODUCTION

Malignant glioma is one of the most common primary brain tumors with drastically poor prognosis[1]. Recently, isocitrate dehydrogenase (IDH) mutation status has been used as the hallmark for glioma diagnosis due to its profound effects on tumor metabolism and subsequent epigenetic dysregulation[2–4]. IDH-mutant (IDH-Mut) gliomas differ from IDH-wild type (IDH-WT) gliomas in many aspects, including tumor growth, invasive capacity, as well as the composition of tumor microenvironment and tissue stiffness[5,6].

Tissue stiffness, one of tumor's physical features, is drawing broader attention. Tissue stiffness is closely associated with tumor progression and recurrence[7,8]. Increased stiffness promotes glioblastoma (GBM) aggression[9]. The extracellular matrix (ECM) is a major contributors to tissue stiffness due to its capacity to form special fibrous network structures, sheet-like networks, and viscous anti-stress networks in specific tissues[8]. In tumors, the biochemical, biomechanical, architectural, and topographical characteristics of the ECM differ from those of normal tissues[10]. Accumulation of fibrous proteins, such as collagen and hyaluronan, increases tumor stiffness and promotes tumor proliferation and migration[11]. An in vitro study showed that synthesizing ECM-cross-linked hydrogels of different stiffness also affect the migration and proliferation of gliomas[12]. A recent study suggested that IDH-WT gliomas exhibited higher stiffness than IDH-Mut gliomas[9]. Nonetheless, the underlying mechanism is not well elucidated.

Tissue inhibitor of metalloproteinase-1 (TIMP1) functions as an inhibitor of matrix metalloproteinases (MMPs) to remodel the ECM. TIMP1 inhibits metalloproteinases and interacts with cell surface proteins, thereby remodeling extracellular matrix proteins and initiating a wide range of downstream effects[13]. Zhao et al. demonstrated that substrate stiffness regulates the activities of MMPs and TIMPs[14], which modulates the migratory and invasive abilities of adenoid cystic carcinoma cells via the RhoA/ROCK pathway. TIMP1 was also found to promote glioblastoma growth and was proposed as a prognostic marker[15]. However, in gliomas with different IDH mutant status, the relationship between TIMP1 and stiffness remains unknown. In this study, we aimed to investigate the relationship between TIMP1 expression and stiffness in IDH-WT and IDH-Mut gliomas.

MATERIALS AND METHODS

Cell culture

Primary glioblastoma cell 1016B was isolated from primary glioblastoma tissue according to a well-established glioblastoma specimen dissociation protocol[16]. 1016B and glioblastoma cell line LN229 were grown in DMEM supplemented with 10% fetal bovine serum (Gibco, Thermo Fisher, USA) and

[1]Institute of Pathology and Southwest Cancer Center, Southwest Hospital, Third Military Medical University (Army Medical University) and Key Laboratory of Tumor Immunopathology, Ministry of Education of China, Chongqing 400038, China. ✉email: bianxiuwu@263.net; pingyifang@126.com

Received: 18 October 2021 Revised: 24 June 2022 Accepted: 27 June 2022
Published online: 26 July 2022

100 units ml^{-1} penicillin/streptomycin (Gibco, Thermo Fisher, USA). To construct IDH1-mutant cell lines, human IDH1-R132H mutant cDNA was generated and inserted into a lentivirus vector (Genechem, China), followed by transduction into IDH1-wild type cells. IDH1-wild type cells transduced with the empty lentivirus vector were used as negative control. The cells were then under puromycin (Gibco, Thermo Fisher, USA) selection.

Glioma samples

Glioma samples were obtained from the Biobank of the Southwest Hospital, Third Military Medical University (TMMU), ranging from January 2016 to June 2021. All human specimens used in this study were approved by the Ethics Committee of Southwest Hospital, TMMU, and informed consent was obtained from patients or their guardians. All the procedures were performed in accordance with the principles of the Declaration of Helsinki. The pathological diagnoses of gliomas were made by two neuropathologists according to the fifth WHO classification of CNS tumors[2]. Tissue stiffness-related differential genes were identified by overlapping three gene sets, including the ECM protein gene set[17,18], stiffness-related gene set (GSE95680, 4.6 kPa vs. 200 kPa)[19], and differential genes in gliomas with different IDH mutation status from TCGA database (http://cancergenome.nih.gov). R software was used to analyze the differentially expressed genes between groups. Differentially expressed genes between IDH1-WT vs. IDH1-Mut gliomas in TCGA database, and ECM gene set in GO database were overlapped with a parameter ($P < 0.05$, $|\text{LogFC}| > 0.58$). Venn diagram was plotted to illustrate the common genes of the three differentially expressed gene sets. Glioma gene expression datasets from TCGA and CGGA (http://www.cgga.org.cn/) were used to analyze the expression of the ECM-related genes and prognostic significance of *TIMP1*.

Atomic force microscopy

The structural feature of every glioma tissue was identified by two neuropathologists in glioma tissue sections stained with H&E staining. Histologically, the tumor cell-enriched area is defined as the nuclei-enriched area, in which the ratio of tumor cell number to tumor-adjacent cell number is about ~500:1. The vessel-enriched area is marked by increased density of blood vessels with thickened walls (endothelial cell and pericyte proliferation). Necrotic area is marked by disintegrating nuclei surrounded by pseudopalisading cells. Tumor-invasive front is the border zone between the tumor cell enrichment area and the non-tumor area. Non-tumor area refers to peritumoral brain tissue. The above-mentioned five regions from three cases of GBMs were subjected to stiffness measurement. Five to eight fields of every region in each case were selected, and 25 points of each field were chosen randomly for evaluating the tissue stiffness of different areas. When the probe detects an empty point, the value is null.

Tissue stiffness was measured using a Nano Wizard II atomic force microscope (AFM, JPK, Nanowizard II BioAFM, Germany). The standard spherical polystyrene cantilever had a 2 μm diameter, and the spring constant of 0.1 N m^{-1} was connected to the AFM system. One of the 20 μm frozen glioma continuous sections was observed using an inverted optical microscope. Once the section was located, the cantilever was carefully moved to the top of the tissue. All mechanical measurements were performed at room temperature (20 °C to 25 °C) in a saline solution. Hematoxylin-eosin (H&E) staining were performed on continuous sections from the same tissue, and the whole slide images of H&E slides were captured using a Pannoramic MIDI scanner (3DHISTECH Ltd., Hungary). The two digital slides were superimposed using the CaseViewer-2.2 software (3DHISTECH Ltd., Hungary), and Adobe Photoshop CC (Adobe Systems) was used to identify the tissue position. Force curves were analyzed using the JPK software (JPK, Germany). Elasticity is a property of a material that characterizes its ability to resist deformation and denotes the stiffness of cells and tissues. Elasticity is represented by Young's modulus with pressure unit Pascal (Pa). The higher the Young's modulus, the harder the corresponding object is (the less elastic it is)[20].

Immunofluorescence staining

Six micrometer-thick glioma frozen sections were fixed with 4% paraformaldehyde for 15 min at room temperature and washed with phosphate-buffered saline (PBS) three times for 5 min each time. The sections were then blocked with a buffer consisting of 1% bovine serum albumin (BSA) in PBS for 60 min at 37 °C, followed by incubation with primary antibody overnight at 4 °C. The sections were then washed three times in PBS and incubated with goat anti-rabbit Dylight™ 555 (1:500, A32732, Thermo Fisher Scientific) or goat anti-mouse Dylight™ 647 (1:500, A32728, Thermo Fisher Scientific) for 1 h at room temperature. After washing in PBS three times, the sections were incubated with DAPI working buffer for 15 min, washed three times with PBS, and mounted with a fluorescent anti-quenching mounter. The sections were observed and images were acquired using a LSM900 confocal system scanning microscope (Zeiss, Jena, Germany). The primary antibodies used in this study were fibronectin (FN) (1:200, ab2413, Abcam), tenascin C (TNC) (1:100, ab108930, Abcam), PTPRZ1 (1:250, 610179, BD Biosciences) and TIMP1 (1:200, ab211926, Abcam). Image J software was used to measure the fluorescence intensity and the number of cells in the image. The fluorescence intensity was divided by the number of cells to obtain the average fluorescence intensity of each image.

Western blot

Western blot was carried out under a standard protocol as used previously[16]. Primary antibodies were IDH1-R132H (1:1000, DIA-H09, Dianova, Germany), MT1-MMP (1:1000, #13130, CST), MMP2 (1:1000, #87809, CST) and GAPDH (1:1000, #5174, CST).

Methylation-specific polymerase chain reaction (MS-PCR)

MS-PCR was used to determine the methylation status of *TIMP1* gene promoter. Briefly, genomic DNA of IDH-WT and IDH-Mut cells was extracted using a Genomic DNA Extraction Kit (#DP304, TIANGEN, China) in K2EDTA tubes. DNA (500 ng) was then subjected to bisulfite modification using a DNA Bisulfite Conversion Kit (DP215, TIANGEN, China), and was used to determine the methylation status of *TIMP1* promoter by MS-PCR using a Methylation-specific PCR Kit (EM101; TIANGEN, China). The primer sequences were below. M-forward, AGATTTTAGGGGATTGGGTC; M-reverse, AAAATAAA-TATCCACGCTAAAAACG; U-forward, GAGATTTTAGGGGATTGGGTT; U-reverse, ATAAATATCCACACTAAAAACAAAA.

Establishment of intracranial glioma xenograft model

All animal experiments were approved by the Institutional Animal Care and Use Committee of TMMU in accordance with the Guide for the Care and Use of Laboratory Animals. IDH1-WT glioma cells were infected with the Ubi-MCS-3FLAG-CMV-EGFP-puromycin lentiviral vector carrying IDH1-R132H as previous described[21] to construct IDH1-Mut glioma cell line. TIMP1 was knocked down with the pHBLV-U6-MCS-CMV-ZsGreen-PGK-puromycin lentiviral vector carrying shRNA of TIMP1 in IDH1-WT glioma cells. Twenty thousand IDH1-Mut glioma cells, IDH-WT glioma cells, TIMP1 knockdown glioma cells or the matched control cells expressing luciferase reporter gene were transplanted into the right frontal lobe of NOD-SCID mice ($n = 10$). Xenograft tumor growth was monitored using AniView100 Multi-mode In vivo Animal Imaging System (Biolight Biotechnology, China) at the indicated intervals. All mice were euthanized on day 22 and fresh brain tissue was collected and subjected to stiffness detection by atomic force microscope, or fixed with 4% paraformaldehyde for immunofluorescence staining. The shRNA sequence was as follows: Scrambled sequence: TTCTCCGAACGTGTCACGTAA, shRNA1 sequence: CTGTTGTTGCTGTGGCTGATA, shRNA2 sequence: GAAGTCAACCAGACCACCTTA.

Statistical analysis

GraphPad Prism (version 7.0) was used for statistical analyses. Data are presented as mean ± SE. One-way ANOVA analysis was applied for multi-group data, and Student's *t*-test (two-tailed) was used for the comparison between two groups. Pearson's correlation analysis was used to analyze the correlation between the average stiffness and the average relative fluorescence intensity of TIMP1 in glioma tissue, the correlation between *TIMP1* expression and *FN* or *TNC* expression in CGGA database. Fisher's exact test was used to analyze the correlation between the tissue stiffness with clinicopathological parameters of glioma samples. X-tile software (Rimm Lab, Yale University) was used to obtain the best cut-off value for Log-rank survival analyses and Kaplan-Meier plots. *P* value less than 0.05 was considered as statistically significant for all analyses.

RESULTS

IDH-WT gliomas showed more tissue stiffness than IDH-Mut gliomas

Thirty-seven adult-type diffuse glioma specimens were analyzed for evaluation of tissue stiffness (Supplementary Table S1). Due to

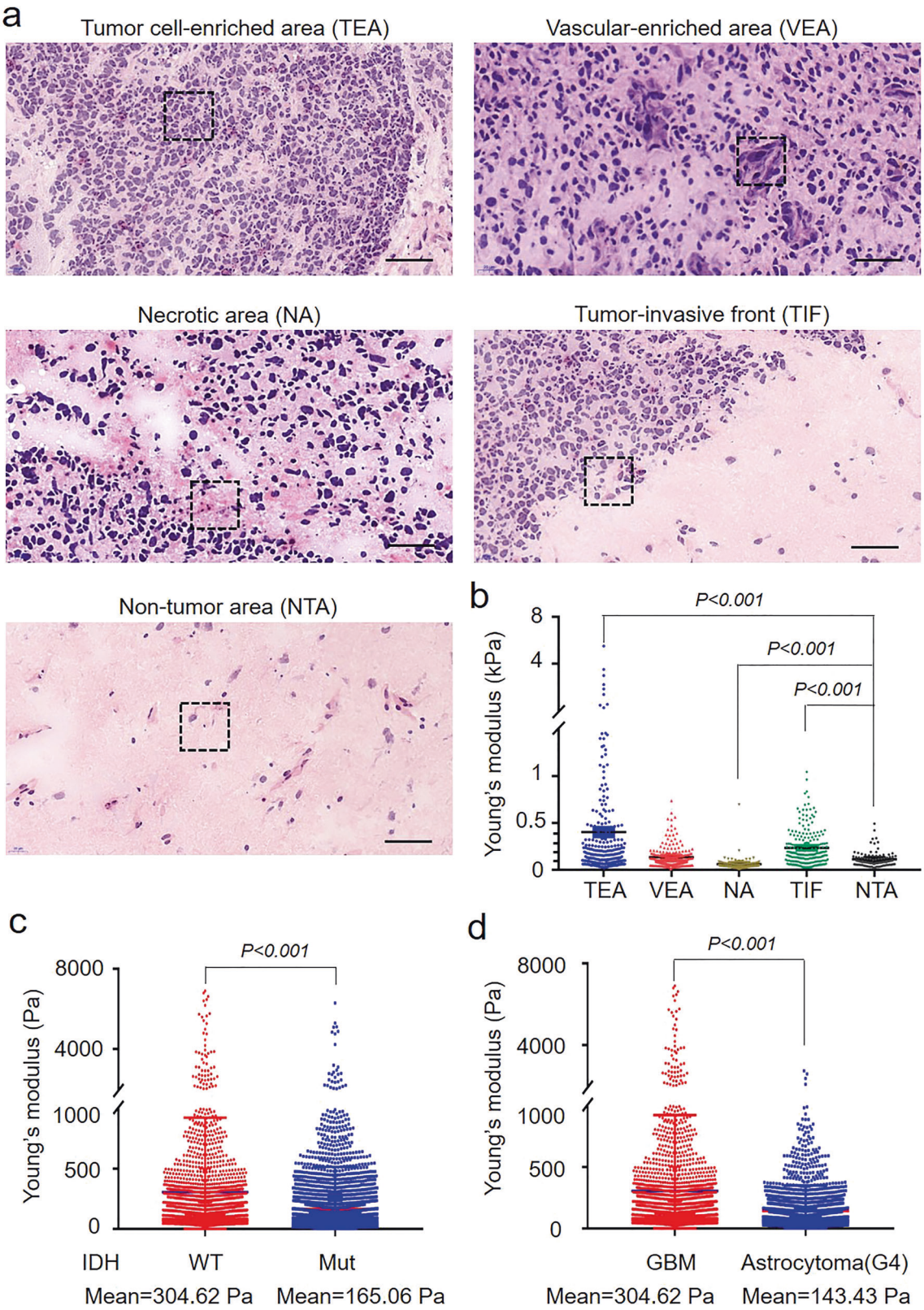

Fig. 1 IDH-WT gliomas showed increased stiffness compared to IDH-Mut gliomas. a Typical H&E images of different areas in glioblastoma sample, including the tumor cell-enriched area (TEA), vascular-enriched area (VEA), necrotic area (NA), tumor-invasive front (TIF) and non-tumor area (NTA). The black dotted box represents the tissue stiffness detection area of 50 × 50 μm. Bars = 50 μm. **b** Quantitative analysis of the tissue stiffness in 350 points of each area in glioblastoma ($n = 3$). **c** Comparison of tissue stiffness in IDH-WT gliomas ($n = 16$) and IDH1-Mut gliomas ($n = 21$). Five to eight regions in tumor cell enrichment area of each glioma samples were measured by AFM. **d** Comparison of the tissue stiffness in tumor cell enrichment area between IDH-WT GBM ($n = 16$) and astrocytoma (Grade 4) ($n = 10$). Pa refers to Pascal.

Table 1. Correlation of tissue stiffness with clinicopathological parameters of glioma samples.

Glinicopathological parameters	*n*	High stiffness (*n*)	Low stiffness (*n*)	*P* value
IDH1/2				
WT	16	12	4	0.008
Mut	21	6	15	
Age				
≥40	28	17	11	0.018
<40	9	1	8	
Pathological diagnosis				
Glioblastoma	16	12	4	<0.001
Oligodendroglioma	8	6	2	
Astrocytoma	13	0	13	
Gender				
Male	24	12	12	ns
Female	13	6	7	

IDH isocitrate dehydrogenase, *WT* wildtype; *Mut* mutation.

the heterogeneity of gliomas, we first measured the stiffness of different regions in each glioblastoma section, including tumor cell-enriched area, vessel-enriched area, necrotic area, tumor-invasive front and non-tumor area (Fig. 1a). The average stiffness of the tumor cell-enriched area was 402.67 Pa, which was obviously higher than that of the non-tumor area (111.61 Pa) (Fig. 1b). The stiffness of the vascular-enriched area was similar with that of the non-tumor area, with an average stiffness of 133.2 Pa. The necrotic area showed the lowest stiffness, with an average stiffness of 59.18 Pa. Stiffness in the tumor-invasive front was also higher than that in the non-tumor area (232.68 Pa vs 111.61 Pa). These results suggest that the stiffness within the glioma tissue was positively correlated with tumor cell enrichment level. Next, we analyzed the tumor tissue stiffness in the tumor cell enrichment areas of 37 cases of gliomas (Table 1) and found that the stiffness of IDH-WT gliomas was significantly higher than that of IDH-Mut gliomas, with the mean stiffness 304.62 Pa of IDH-WT gliomas and 165.06 Pa of IDH-Mut gliomas, respectively (Fig. 1c). In addition, the stiffness of IDH-WT glioblastomas was higher than that of IDH-Mut astrocytoma (WHO grade 4) (Fig. 1d). Taken together, the stiffness of gliomas is heterogeneous, and the tumor cell enrichment area of IDH-WT glioblastomas possesses hardest tissue stiffness.

TIMP1 was highly expressed in IDH-WT gliomas

As ECM is a crucial contributor to tissue stiffness, we next analyzed the potential molecules contributing to the increased ECM stiffness in IDH-WT gliomas. As shown in Venn diagram, 16 ECM-stiffness-related genes were shown overlapping in three gene sets including stiffness-related gene set (GSE95680), the differentially expressed genes between IDH1-WT *vs*. IDH1-Mut gliomas in TCGA database, and ECM gene set in GO database ($P < 0.05$, $|\text{LogFC}| > 0.58$) (Fig. 2a). Among these genes, the fold change of *TIMP1* gene expression was the most differential between IDH-WT and IDH-Mut gliomas (Fig. 2b). In TCGA database, *TIMP1* expression was higher in IDH-WT gliomas compared with IDH-Mut gliomas (Fig. 2c). To further verify this, the expression levels of *TIMP1* in the Chinese Glioma Genome Atlas (CGGA) database was analyzed, and *TIMP1* gene expression was significantly higher in IDH-WT gliomas than that in IDH-Mut gliomas, independent of tumor grade (Fig. 2d). In addition, glioma patients with high *TIMP1* expression had significantly worse survival than those with low *TIMP1* expression in IDH-WT gliomas (Fig. 2e–g). To verify the above results, we detected the expression of TIMP1 protein in IDH-WT and IDH-Mut gliomas by immunofluorescence staining. Consistently, TIMP1 protein was more highly expressed in IDH-WT glioblastomas than IDH-Mut astrocytoma (G4) (Fig. 2h, i). Taken together, these data demonstrate that TIMP1 is highly expressed and may be related to the increased stiffness in IDH-WT gliomas.

TIMP1 expression was positively correlated with glioma stiffness

To define the relationship between TIMP1 expression and glioma stiffness, the correlation index of TIMP1 and tissue stiffness was evaluated. A significant positive correlation between glioma stiffness and TIMP1 expression was found (Fig. 3a). As TIMP1 mainly functions as a MMP inhibitor, and tenascin C and fibronectin are the targets of MMP-mediated degradation, and key contributors to tissue stiffness of glioma, we then evaluated the correlation between *TIMP1* and *TNC*/*FN* genes. *TIMP1* expression was positively correlated with the expression of *TNC* and *FN* in 651 gliomas from CGGA database (Fig. 3b, c). Immunofluorescence staining confirmed that the expression of tenascin C and fibronectin in IDH-WT glioblastomas were higher than in IDH-Mut astrocytoma (G4) (Fig. 3d, e). Additionally, IDH-WT gliomas showed more prominent extracellular expression of fibronectin and tenascin-C than IDH-Mut gliomas when co-staining with glioma tumor cell marker PTPRZ1 (Fig. 3d).

By methylation database analysis (http://www.cgga.org.cn/analyse/Methyl-data.jsp), we found that the degree of DNA methylation of *TIMP1* in IDH-WT gliomas was significantly lower than that in IDH-Mut gliomas (Fig. 3f). By introducing IDH1-R132H vectors into human IDH1-wild type glioma cells to obtain an IDH1-mutant cell line, we found that the introduction of IDH1-R132H mutation significantly increased the degree of DNA promoter methylation of *TIMP1* as compared to IDH-WT glioblastoma cells as revealed by methylation-specific PCR (Fig. 3g), suggesting that high TIMP1 expression in IDH-WT gliomas might be attributed to the low DNA methylation on its promoter region. These results suggest that the high levels of TIMP1 lead to increased stiffness in IDH-WT glioblastomas.

TIMP1 knockdown decreased tissue stiffness and the expression of fibronectin and tenascin C in IDH1-WT glioma xenograft

Using the primary glioma cells carrying IDH1-R132H mutants or empty (IDH-WT) vectors (Fig. 4a), we next established an orthotopic glioma xenograft model. Bioluminescence imaging showed that IDH1-WT glioma xenografts grew significantly

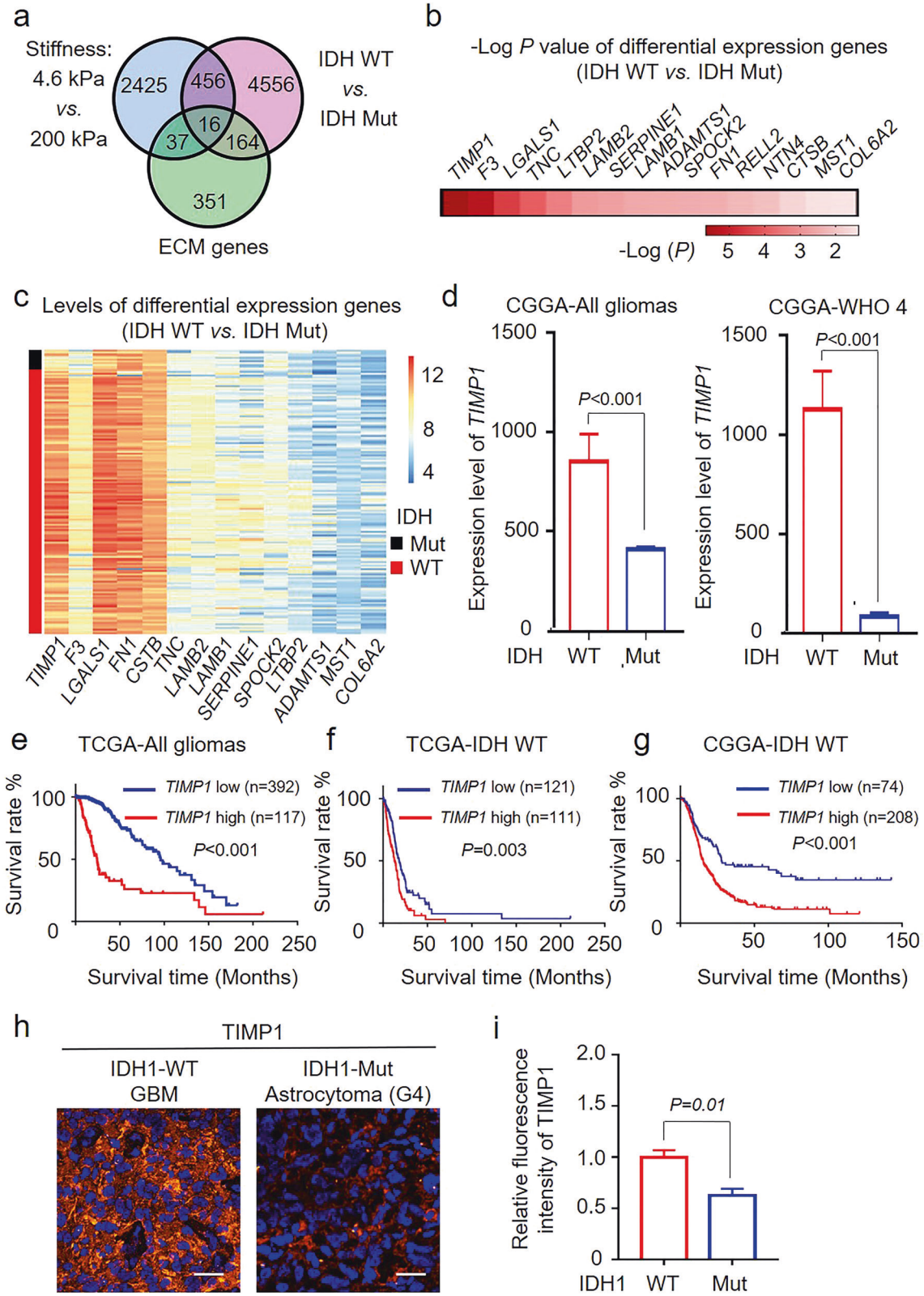

Fig. 2 TIMP1 was highly expressed in IDH-WT gliomas and predicted poor prognosis. a The Venn diagram revealed that 16 differential genes overlapped in three genes sets, including ECM gene set, differential genes in stiffness-related gene set and differential genes in DH-WT and IDH-Mut glioma from TCGA glioma database. **b** The Log P value of 16 differential expressed genes. **c** Heatmap of the 16 genes expression in IDH-WT and IDH-Mut gliomas from TCGA database. **d** *TIMP1* expression in gliomas with different IDH status in the CGGA database. Data were presented as mean ± SE. **e**–**g** Kaplan–Meier survival analysis of glioma patients with different *TIMP1* expression in all gliomas in TCGA database (**e**), IDH-WT gliomas in TCGA (**f**) and CGGA database (**g**). **h** Typical images of TIMP1 in IDH-WT glioblastoma and IDH-Mut astrocytoma (Grade 4). Bars = 20 μm. **i** Relative fluorescence intensity of TIMP1 in IDH-WT glioblastoma ($n = 16$) and astrocytoma (Grade 4) ($n = 10$). Data were presented as mean ± SE.

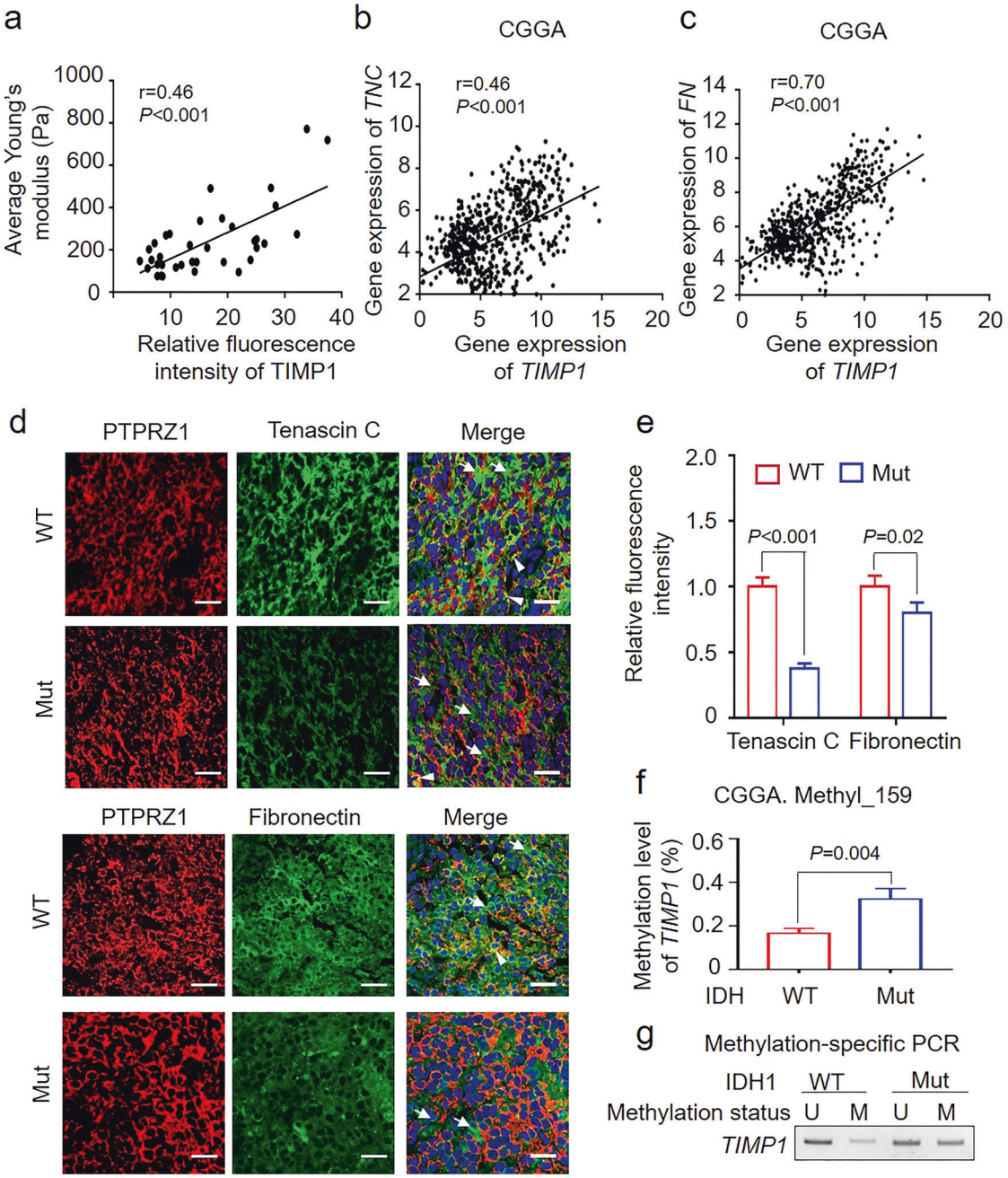

Fig. 3 TIMP1 is positively correlated with tissue stiffness and stiffness-related molecules. a Correlation analysis of average Young's modulus and relative fluorescence intensity of TIMP1 ($n = 37$). **b**, **c** Correlation analysis of *TIMP1* and stiffness-related molecules *TNC* (tenascin C) (**b**) and *FN* (fibronectin) (**c**) from CGGA database. **d** Typical images of PTPRZ1, tenascin C, and fibronectin in IDH-WT glioblastoma and IDH-Mut astrocytoma (Grade 4). The white arrow indicates the green color-only signals (fibronectin-positive or tenascin-C-positive), the white arrowhead indicates the orange color signals (fibronectin-positive or tenascin-C-positive plus PTPRZ1-positive). Bars = 20 μm. **e** Relative fluorescence intensity of tenascin C and fibronectin in IDH-WT glioblastoma ($n = 16$) and IDH-Mut astrocytoma (Grade 4) ($n = 10$). Data were presented as mean ± SE. **f** Methylation level of *TIMP1* in IDH-WT and IDH-Mut gliomas in CGGA database. Data were presented as mean ± SE. **g** Methylation-specific PCR of *TIMP1* in IDH1-WT and IDH1-Mut glioma cells in triplicate repeats. M methylation, U unmethylated.

faster than the IDH1-Mut glioma (Fig. 4b, c). Immunofluorescence staining of frozen sections of tumor xenografts confirmed that IDH1-WT gliomas expressed higher levels of TIMP1, fibronectin and tenascin C than gliomas with IDH1-R132H mutants (Fig. 4d, e). Consistently, the stiffness of IDH1-WT glioma xenografts was obviously higher than that of gliomas with IDH1-R132H mutants (Fig. 4f). To further confirm the roles of TIMP1 in mediating glioma stiffness in xenografts, we performed in vivo loss of function analysis by establishing intracranial glioma xenografts using glioma cells transduced with TIMP1 short hairpin RNAs or control constructs. Immunofluorescence staining of TIMP1 with fibronectin or tenascin C on tumor xenograft sections showed that the expression of both fibronectin and tenascin C were significantly decreased in TIMP1-knockdown glioma (Fig. 4g, h). Similarly, the stiffness of TIMP1-knockdown glioma xenograft tissue was also lower than that of control group (Fig. 4i). In addition, knockdown of TIMP1 in glioma cell line and primary glioma cells in vitro increased the

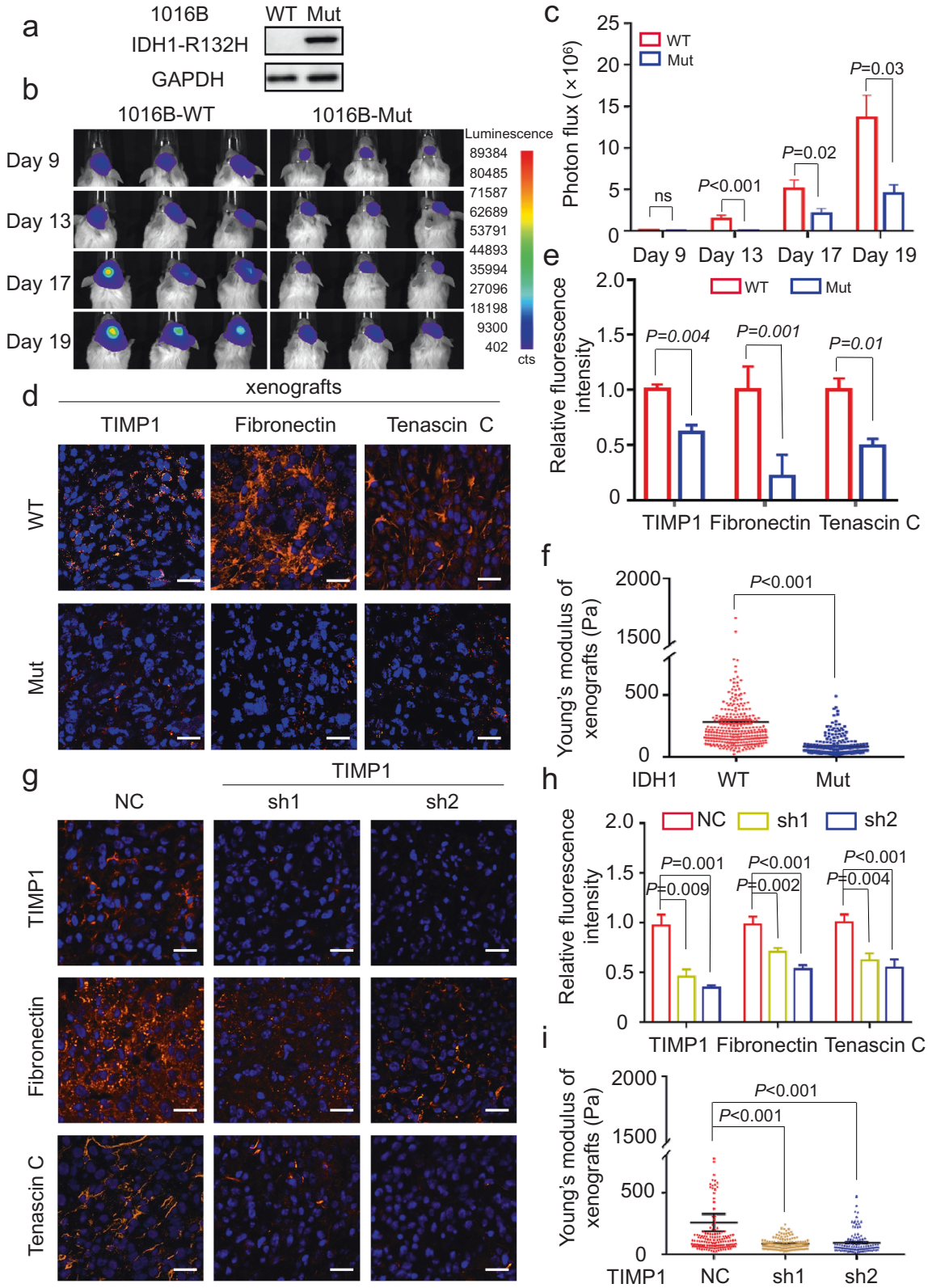

expression of MT1-MMP and MMP2, two MMPs for fibronectin and tenascin C degradation (Supplementary Fig. 1a–d). Conclusively, these data indicate that knockdown of TIMP1 decreases glioma tumor stiffness through downregulating fibronectin and tenascin C expression.

DISCUSSION

In this study, we demonstrated that TIMP1 was highly expressed in IDH-WT glioblastoma and was positively correlated with the increased tissue stiffness. Several studies reported the close relationship between molecules involved in stiffness regulation

Fig. 4 High expression of TIMP1 affects the tissue stiffness in glioma orthotopic xenografts. a Immunoblot analysis of IDH1-R132H in IDH1-WT and IDH1-Mut glioma cells in triplicate repeats. **b**, **c** Representative bioluminescent images (**b**) and the quantification (**c**) of IDH1-WT and IDH1-Mut glioma xenografts with 10 mice in each group. Data were presented as mean ± SE. **d** Typical images of TIMP1, fibronectin and tenascin C in IDH1-WT and IDH1-Mut glioma xenografts. Bars = 20 μm. **e** Relative fluorescence intensity of TIMP1, fibronectin and tenascin C in IDH1-WT and IDH1-Mut glioma xenografts (each group $n = 6$). Data were presented as mean ± SE. **f** Young's modulus of IDH1-WT and IDH1-Mut glioma xenografts in tumor cell enrichment area (each group $n = 3$). **g** Typical images of TIMP1, fibronectin, and tenascin C in glioma xenografts derived from TIMP1 knockdown IDH1-WT glioma cells and control cells in xenografts. Bars = 20 μm. **h** Relative fluorescence intensity of TIMP1, fibronectin, and tenascin C in glioma xenografts derived from TIMP1 knockdown IDH1-WT glioma cells and control cells (each group $n = 6$). Data were presented as mean ± SE. **i** Young's modulus of TIMP1 knockdown xenografts and control xenografts (each group $n = 3$).

and glioma progression. For example, stiffness-regulating protein PIEZO1 was highly expressed in GBM and promoted GBM progression[22]. MGAT5 regulated glioma stiffness and promoted the invasion of glioma cells[23]. Notably, our study clarifies a TIMP1-mediated tumor stiffness regulation in a manner dependent on IDH1 mutation status of gliomas, which provides a new link between IDH mutation and glioma biomechanical characteristics. Since the stiffness of IDH-WT gliomas was higher than that of IDH-Mut gliomas, this study highlights the importance of increased stiffness in the rapid progression of IDH-WT gliomas.

Stiffness contributes to tumor progression. Previous studies have reported that increased stiffness promoted tumor cell proliferation and invasion, resulting in tumor progression[8,24]. Decreasing tumor stiffness by the renin-angiotensin system inhibitor could inhibit tumor metastases[25]. Our study demonstrates that TIMP1 may be another promising therapeutic target for malignant gliomas through promoting glioma stiffness and predicting poor prognosis of glioma patients.

It is reported that the stiffness of some solid tumors, such as breast cancer [26,27], liver cancer[28] and prostate cancer[29], are higher than that of gliomas. For example, the stiffness of breast cancer and liver cancer is more than 1kPa and 6 kPa, respectively. In view of this, we detected the stiffness of breast cancer by atomic force microscopy and found that the stiffness of tumor cell-enriched area of breast cancer was higher than that of glioma (data not shown). The possible reason is that there is more fibrous tissue in breast cancer than that in glioma. Furthermore, the stiffness of normal brain is significantly softer than other tissue. It should be mentioned that the change of tissue stiffness in tumor microenvironment is a pivotal hallmark of solid tumors[22]. Our study demonstrated that tissue stiffness of tumor cell-enriched area was significantly higher than that in non-tumor area, indicating that a "stiff" microenvironment formed in glioma rather than normal brain tissue. Tumor tissue stiffness is determined by the cells and ECM components in tumor microenvironment[27,30]. Tumor cells and activated stromal cells secrete a large quantity of proteases and growth factors to regulate the secretion, degradation, and recombination of the ECM[17,31]. In combination with our results, this study provides clear evidence that glioma cells are the major contributor of glioma stiffness.

Our study demonstrates that TIMP1 is more highly expressed in IDH-WT gliomas than in IDH-Mut gliomas. TIMP1 is an endogenous inhibitor of MMPs that inhibits at least 14 metalloproteinases in the brain tissues[13,32]. MMPs degrades ECM and are involved in many tumoral pathophysiological processes such as tumor angiogenesis and metastasis[33,34]. Based on that finding, TIMP1 may regulate tissue stiffness by inhibiting ECM degradation. Fibronectin and tenascin C are the major substrate of various metalloproteinases. MT1-MMP regulates fibronectin remodeling through degrading extracellular fibronectin and enhancing endocytosis[35]. MMP-2 catalyzes TNfnA2 domain of tenascin C to change stress fibers and focal adhesion sites[36–38]. TIMP1 expression levels were positively correlated with the expression levels of fibronectin and tenascin C in IDH-WT gliomas, suggesting that TIMP1 might increase tissue stiffness by inhibiting metalloproteinases and promoting the accumulation of fibronectin and tenascin C.

We found that the degree of TIMP1 promoter methylation was significantly lower in IDH-WT gliomas than that in IDH-Mut gliomas. In glioma, the IDH mutation leads to 2-hydroxyglutaric acid accumulation and inhibits TET-catalyzed 5mC to 5hmC conversion, resulting in the alteration of DNA methylation[39]. TIMP1 expression is repressed in IDH-mutant glioma by increased promoter methylation, which could be rescued by 5-aza-2′-deoxycytidine[40,41]. Therefore, low promoter methylation level of TIMP1 results in an increased TIMP1 expression in IDH-WT gliomas. TIMP1 expression might also be affected by other factors. In diffuse large B-cell lymphoma, TIMP1 expression is inhibited by siRNA targeting the ECM protein fibrillin 1[42]. In a high-glucose trauma environment, macrophage-derived TNFα regulated TIMP1 expression to impair keratinocyte migration[43]. In addition, histone deacetylase 1 (HDAC1) can suppress TIMP1 transcriptional activation to improve vascular structure[44]. Whether these mechanisms are involved in the upregulation of TIMP1 in IDH-WT gliomas needs further exploration.

Our results indicate that TIMP1 acts as a prognostic biomarker for glioma, in agreement with previous studies on cercical cancer[45], ovarian cancer[46], and colorectal cancer[47]. TIMP1 binds to its cell surface binding partner CD63 and activates ERK signaling to induce neutrophil extracellular trap formation and tumor progression in highly fatal pancreatic cancer[48]. In human neural stem cells, TIMP1 and CD63 induce Akt and FAK phosphorylation to activate β1 integrin-mediated signal transduction and alter the distribution of vinculin and F-actin[49]. In various types of cancer cells, TIMP1 activates YAP/TAZ signaling and promotes the proliferation of tumor cells[31,50]. YAP/TAZ signaling is critical for transmitting the mechanical signal to the nucleus[51], indicating the potential role of TIMP1-induced YAP/TAZ activation in stiffness-mediated glioma progression. TIMP1 knockdown reduced the stiffness of IDH-WT glioma transplants, highlighting the therapeutic significance of TIMP1 in IDH-WT gliomas.

DATA AVAILABILITY

The authors confirm that the data supporting the findings of this study are available within the article or its supplementary materials.

REFERENCES

1. Zhang, L., He, L., Lugano, R., Roodakker, K., Bergqvist, M., Smits, A. et al. IDH mutation status is associated with distinct vascular gene expression signatures in lower-grade gliomas. *Neuro Oncol* 20, 1505–1516 (2018).
2. Louis, D. N., Perry, A., Wesseling, P., Brat, D. J., Cree, I. A., Figarella-Branger, D. et al. The 2021 WHO Classification of Tumors of the Central Nervous System: A summary. *Neuro Oncol* 23, 1231–1251 (2021).
3. Ng, H., Wong, Q. H., Liu, E. M., Li, K. K. The new WHO molecular criteria for adult glioblastoma – Are we a step too far? *Glioma* 4, 65–67 (2021).
4. Yang, R., Zhao, Y., Gu, Y., Yang, Y., Gao, X., Yuan, Y. et al. Isocitrate dehydrogenase 1 mutation enhances 24(S)-hydroxycholesterol production and alters cholesterol homeostasis in glioma. *Oncogene* 39, 6340–6353 (2020).
5. Waitkus, M. S., Diplas, B. H., Yan, H. Biological role and therapeutic potential of IDH mutations in cancer. *Cancer Cell* 34, 186–195 (2018).

6. Pirozzi, C. J., Yan, H. The implications of IDH mutations for cancer development and therapy. *Nat Rev Clin Oncol* 18, 645–661 (2021).
7. Levental, K. R., Yu, H., Kass, L., Lakins, J. N., Egeblad, M., Erler, J. T. et al. Matrix crosslinking forces tumor progression by enhancing integrin signaling. *Cell* 139, 891–906 (2009).
8. Bonnans, C., Chou, J., Werb, Z. Remodelling the extracellular matrix in development and disease. *Nat Rev Mol Cell Biol* 15, 786–801 (2014).
9. Miroshnikova, Y. A., Mouw, J. K., Barnes, J. M., Pickup, M. W., Lakins, J. N., Kim, Y. et al. Tissue mechanics promote IDH1-dependent HIF1alpha-tenascin C feedback to regulate glioblastoma aggression. *Nat Cell Biol* 18, 1336–1345 (2016).
10. Cox, T. R. The matrix in cancer. *Nat Rev Cancer* 21, 217–238 (2021).
11. Unnikandam, V. S., Hwang, D., Correia, J., Bartlett, M. D., Schneider, I. C. Cancer cell migration in collagen-hyaluronan composite extracellular matrices. *Acta Biomater* 130, 183–198 (2021).
12. Dou, J., Mao, S., Li, H., Lin, J. M. Combination stiffness gradient with chemical stimulation directs glioma cell migration on a microfluidic chip. *Anal Chem* 92, 892–898 (2020).
13. Grunwald, B., Schoeps, B., Kruger, A. Recognizing the molecular multifunctionality and interactome of TIMP-1. *Trends Cell Biol* 29, 6–19 (2019).
14. Zhao, D., Li, Q., Liu, M., Ma, W., Zhou, T., Xue, C. et al. Substrate stiffness regulated migration and invasion ability of adenoid cystic carcinoma cells via RhoA/ROCK pathway. *Cell Prolif* 51, e12442 (2018).
15. Guo, Y., Wang, X., Ning, W., Zhang, H., Yu, C. Identification of two core genes in glioblastomas with different isocitrate dehydrogenase mutation status. *Mol Biol Rep* 47, 7477–7488 (2020).
16. Zhang, X. N., Yang, K. D., Chen, C., He, Z. C., Wang, Q. H., Feng, H. et al. Pericytes augment glioblastoma cell resistance to temozolomide through CCL5-CCR5 paracrine signaling. *Cell Res* 31, 1072–1087 (2021).
17. Frantz, C., Stewart, K. M., Weaver, V. M. The extracellular matrix at a glance. *J Cell Sci* 123, 4195–4200 (2010).
18. Dragos, A., Kovacs, A. T. The peculiar functions of the bacterial extracellular matrix. *Trends Microbiol* 25, 257–266 (2017).
19. Bangasser, B. L., Shamsan, G. A., Chan, C. E., Opoku, K. N., Tuzel, E., Schlichtmann, B. W. et al. Shifting the optimal stiffness for cell migration. *Nat Commun* 8, 15313 (2017).
20. Osmulski, P., Mahalingam, D., Gaczynska, M. E., Liu, J., Huang, S., Horning, A. M. et al. Nanomechanical biomarkers of single circulating tumor cells for detection of castration resistant prostate cancer. *Prostate* 74, 1297–1307 (2014).
21. Bunse, L., Pusch, S., Bunse, T., Sahm, F., Sanghvi, K., Friedrich, M. et al. Suppression of antitumor T cell immunity by the oncometabolite (R)-2-hydroxyglutarate. *Nat Med* 24, 1192–1203 (2018).
22. Chen, X., Wanggou, S., Bodalia, A., Zhu, M., Dong, W., Fan, J. J. et al. A feedforward mechanism mediated by mechanosensitive ion channel PIEZO1 and tissue mechanics promotes glioma aggression. *Neuron* 100, 799–815 (2018).
23. Marhuenda, E., Fabre, C., Zhang, C., Martin-Fernandez, M., Iskratsch, T., Saleh, A. et al. Glioma stem cells invasive phenotype at optimal stiffness is driven by MGAT5 dependent mechanosensing. *J Exp Clin Cancer Res* 40, 139 (2021).
24. Fan, Y., Sun, Q., Li, X., Feng, J., Ao, Z., Li, X. et al. Substrate stiffness modulates the growth, phenotype, and chemoresistance of ovarian cancer cells. *Front Cell Dev Biol* 9, 718834 (2021).
25. Shen, Y., Wang, X., Lu, J., Salfenmoser, M., Wirsik, N. M., Schleussner, N. et al. Reduction of liver metastasis stiffness improves response to bevacizumab in metastatic colorectal cancer. *Cancer Cell* 37, 800–817 (2020).
26. Medina, S. H., Bush, B., Cam, M., Sevcik, E., DelRio, F. W., Nandy, K. et al. Identification of a mechanogenetic link between substrate stiffness and chemotherapeutic response in breast cancer. *Biomaterials* 202, 1–11 (2019).
27. Mohammadi, H. Sahai, E. Mechanisms and impact of altered tumour mechanics. Nat Cell Biol 20, 766–774 (2018).
28. Dong, Y., Zheng, Q., Wang, Z., Lin, X., You, Y., Wu, S. et al. Higher matrix stiffness as an independent initiator triggers epithelial-mesenchymal transition and facilitates HCC metastasis. *J Hematol Oncol* 12, 112 (2019).
29. Rouviere, O., Melodelima, C., Hoang, D. A., Bratan, F., Pagnoux, G., Sanzalone, T. et al. Stiffness of benign and malignant prostate tissue measured by shear-wave elastography: A preliminary study. *Eur Radiol* 27, 1858–1866 (2017).
30. Amos, S. E., Choi, Y. S. The cancer microenvironment: Mechanical challenges of the metastatic cascade. *Front Bioeng Biotechnol* 9, 625859 (2021).
31. Karamanos, N. K., Piperigkou, Z., Passi, A., Gotte, M., Rousselle, P., Vlodavsky, I. Extracellular matrix-based cancer targeting. *Trends Mol Med* 27, 1000–1013 (2021).
32. Jackson, H. W., Defamie, V., Waterhouse, P., Khokha, R. TIMPs: Versatile extracellular regulators in cancer. *Nat Rev Cancer* 17, 38–53 (2017).
33. Handsley, M. M., Edwards, D. R. Metalloproteinases and their inhibitors in tumor angiogenesis. *Int J Cancer* 115, 849–860 (2005).
34. Fingleton, B. Matrix metalloproteinases: Roles in cancer and metastasis. *Front Biosci* 11, 479–491 (2006).
35. Shi, F., Sottile, J. MT1-MMP regulates the turnover and endocytosis of extracellular matrix fibronectin. *J Cell Sci* 124, 4039–4050 (2011).
36. Brosicke, N. & Faissner, A. Role of tenascins in the ECM of gliomas. Cell Adh Migr 9, 131–140 (2015).
37. Saito, Y., Imazeki, H., Miura, S., Yoshimura, T., Okutsu, H., Harada, Y., et al. A peptide derived from tenascin-C induces beta1 integrin activation through syndecan-4. *J Biol Chem* 282, 34929–34937 (2007).
38. Echtermeyer, F., Streit, M., Wilcox-Adelman, S., Saoncella, S., Denhez, F., Detmar, M. et al. Delayed wound repair and impaired angiogenesis in mice lacking syndecan-4. *J Clin Invest* 107, R9–R14 (2001).
39. Dang, L., Su, S. M. Isocitrate dehydrogenase mutation and (R)-2-Hydroxyglutarate: From basic discovery to therapeutics development. *Annu Rev Biochem* 86, 305–331 (2017).
40. Ricca, T. I., Liang, G., Suenaga, A. P., Han, S. W., Jones, P. A., Jasiulionis, M. G. Tissue inhibitor of metalloproteinase 1 expression associated with gene demethylation confers anoikis resistance in early phases of melanocyte malignant transformation. *Transl Oncol* 2, 329–340 (2009).
41. Zhang, W., Sun, W., Qin, Y., Wu, C., He, L., Zhang, T. et al. Knockdown of KDM1A suppresses tumour migration and invasion by epigenetically regulating the TIMP1/MMP9 pathway in papillary thyroid cancer. *J Cell Mol Med* 23, 4933–4944 (2019).
42. Wang, H., Liu, Z., Zhang, G. FBN1 promotes DLBCL cell migration by activating the Wnt/beta-catenin signaling pathway and regulating TIMP1. *Am J Transl Res* 12, 7340–7353 (2020).
43. Huang, S. M., Wu, C. S., Chiu, M. H., Wu, C. H., Chang, Y. T., Chen, G. S. et al. High glucose environment induces M1 macrophage polarization that impairs keratinocyte migration via TNF-alpha: An important mechanism to delay the diabetic wound healing. *J Dermatol Sci* 96, 159–167 (2019).
44. Hu, J., Shen, T., Xie, J., Wang, S., He, Y., Zhu, F. Curcumin modulates covalent histone modification and TIMP1 gene activation to protect against vascular injury in a hypertension rat model. *Exp Ther Med* 14, 5896–5902 (2017).
45. Azevedo, M. J., Rabelo-Santos, S. H., Do, A. W. M., Zeferino, L. C. Tumoral and stromal expression of MMP-2, MMP-9, MMP-14, TIMP-1, TIMP-2, and VEGF-A in cervical cancer patient survival: A competing risk analysis. *BMC Cancer* 20, 660 (2020).
46. Abreu, M., Cabezas-Sainz, P., Alonso-Alconada, L., Ferreiros, A., Mondelo-Macia, P., Lago-Leston, R. M. et al. Circulating tumor cells characterization revealed TIMP1 as a potential therapeutic target in ovarian cancer. *Cells* 9, 1218(2020).
47. Barabas, L., Hritz, I., Istvan, G., Tulassay, Z., Herszenyi, L. The behavior of MMP-2, MMP-7, MMP-9, and their inhibitors TIMP-1 and TIMP-2 in Adenoma-Colorectal cancer sequence. *Dig Dis* 39, 217–224 (2021).
48. Schoeps, B., Eckfeld, C., Prokopchuk, O., Bottcher, J., Haussler, D., Steiger, K. et al. TIMP1 triggers neutrophil extracellular trap formation in pancreatic cancer. *Cancer Res* 81, 3568–3579 (2021).
49. Zhang, Z., Lv, J., Lei, X., Li, S., Zhang, Y., Meng, L. et al. Baicalein reduces the invasion of glioma cells via reducing the activity of p38 signaling pathway. *PLoS One* 9, e90318 (2014).
50. Ando, T., Charindra, D., Shrestha, M., Umehara, H., Ogawa, I., Miyauchi, M. et al. Tissue inhibitor of metalloproteinase-1 promotes cell proliferation through YAP/TAZ activation in cancer. *Oncogene* 37, 263–270 (2018).
51. Meng, Z., Qiu, Y., Lin, K. C., Kumar, A., Placone, J. K., Fang, C. et al. RAP2 mediates mechanoresponses of the Hippo pathway. *Nature* 560, 655–660 (2018).

AUTHOR CONTRIBUTIONS

Conception and design: X.-W.B., Y.-F.P., and Y.S. Cell culture: C.-H.L. Staining: C.-H.L., Y.-Q.L., M.L., and J.-Y.M. Immune blotting: C.-H.L., W.-Y.W., H.Z., L.L. Animal experiments: C.-H.L. and M.M. MS-PCR: Q.L. Data analysis: C.C., Q.N., Z.-X.Y., K.-D.Y., and X.-N.Z. Writing of the manuscript: C.-H.L., Y.-F.P., and Y.S.

FUNDING

This research was supported by grants from the National Natural Science Foundation of China (81703012, 81902548), and Science and Technology Innovation Project of Chongqing Science and Technology Commission (cstc2017jcyj-yszxX0012).

COMPETING INTERESTS

The authors declare no competing interests.

ETHICS APPROVAL

The stiffness of human glioma section measuring and human glioma section staining was approved by the Ethics Committees of Southwest Hospital (KY2021041). The animal use was approved by the Ethics Committees of Southwest Hospital (AMUWEC20210594).

ADDITIONAL INFORMATION

Supplementary information The online version contains supplementary material available at https://doi.org/10.1038/s41374-022-00825-4.

Correspondence and requests for materials should be addressed to Xiu-Wu Bian or Yi-Fang Ping.